Impact of dry granular masses on rigid barriers

F Calvetti[1], **C di Prisco**[1] **and E Vairaktaris**[2,3]

[1]Civil and Environmental Department, Politecnico di Milano, Italy
[2] School of Applied Mathematics and Physical Sciences, NTU of Athens, Greece

E-mail: mvairak@mail.ntua.gr

Abstract. This work concerns the impact of dry granular masses on rigid artificial obstacles. The authors approached the problem by performing an extensive campaign of numerical analyses with a commercial code based on the discrete element theory. The standard approaches employed to design sheltering structures are exclusively based on the assessment of the Maximum Impact Force (MIF) exerted by the soil mass on the obstacle, and the sheltering structure is usually designed according to simplified pseudo-static approaches. In a previous paper the authors considered the dependence of MIF on the Froude number and on a large series of both geometrical and mechanical parameters. Indeed, the impulsive nature of the force exerted by the soil onto the structure has to be considered in order to optimize the design of this type of structures. For this reason in this paper the evolution with time of the impact force and the mechanics of the phenomenon are investigated.

1. Introduction

Among the several aspects that have to be considered for landslide risk assessment, the work developed in the last years by the Authors is mainly focussed on the comprehension/modelling of the mechanical processes developing when the landslide interacts with either civil structures or protection works. At present, standard approaches employed to design sheltering structures are exclusively based on the assessment of the Maximum Impact Force (MIF) exerted by the soil mass on the obstacle, since the sheltering structure is usually designed according to simple pseudo-static approaches.

Existing classical approaches employed to design sheltering structures are inspired to:

(i) impacts of fluid masses onto rigid barriers [1], which can be subdivided in hydrostatic (HS) and hydrodynamic (HD);
(ii) impacts of boulders (BI) on elastic walls.

According to HS models ([2],[3], [4]), the MIF value is independent of the soil mass velocity and the pressure is linearly dependent on depth; according to HD models ([3], [4], [5], [6], [7]) the pressure is assumed to be constant with depth and dependent on the average mass velocity. On the other side, the most common BI models ([4], [5], [6], [8], [9]) consider elastic impacts and use the non linear Hertz's equation for the MIF evaluation. In general, hydraulic models provide lower bounds for the MIF, whereas solid impact models estimate upper bound values ([9], [10]).

The literature review clearly shows that numerical codes are not yet very commonly used for this kind of problems. Most of the works approaching this topic by employing numerical codes aim to simulate specific geometrical conditions/cases ([11], [12]). Nevertheless, with the exception of a few

[3] Corresponding author

contributions ([13], [14]), the role played by both geometrical and mechanical factors is not yet investigated in detail.

To analyse the impact of granular masses, the authors decided to employ a DEM code in which the soil mass is simulated as an assembly of rigid spheres with deformable contacts, and the initial conditions for the system are imposed at the instant of time just preceding the impact itself. In a previous work [15], the authors considered the effect of the energetic content, mean velocity, length of the flowing mass (ℓ), flow height (h), front inclination (α), inter-particle (f_c) and ground friction coefficients, mass porosity on the MIF value and they observed that:

1. the total mass impacting on the obstacle is not a representative factor influencing the MIF value. In contrast, the dominant factors are the flow height and the sliding mass porosity.
2. The quantitative dependence of the MIF value on the mean mass velocity seems to depend on the inter-particle friction coefficient,
3. The role of the inter-particle friction angle seems to become irrelevant for large porosities.
4. The inclination of the front plays a dominant role; the largest values of MIF are obtained in case of angles close to 90°.

Finally, in [15] the authors have shown that the Froude number is the main variable to be considered for the assessment of the MIF value and introduced a formula according to which the MIF value can be calculated as a function of all the geometrical and mechanical parameters cited above.

In the current work, in contrast to the previous reference, the authors try to qualitatively describe, from a micro-structural point of view, the mechanical process. The paper is thus organized as it follows. A brief description of the numerical model is given in section 2. For the sake of both clarity and brevity within the enormous number of numerical simulation results obtained by the authors, here below a reference numerical test is only taken into account, since it was considered to be representative. In section 3 the evolution of both force chains and velocity vectors within the soil mass is illustrated. To highlight the mechanical process taking place within the soil mass, three additional numerical tests characterised by different values of the inter-particle friction angle and front inclination are also discussed.

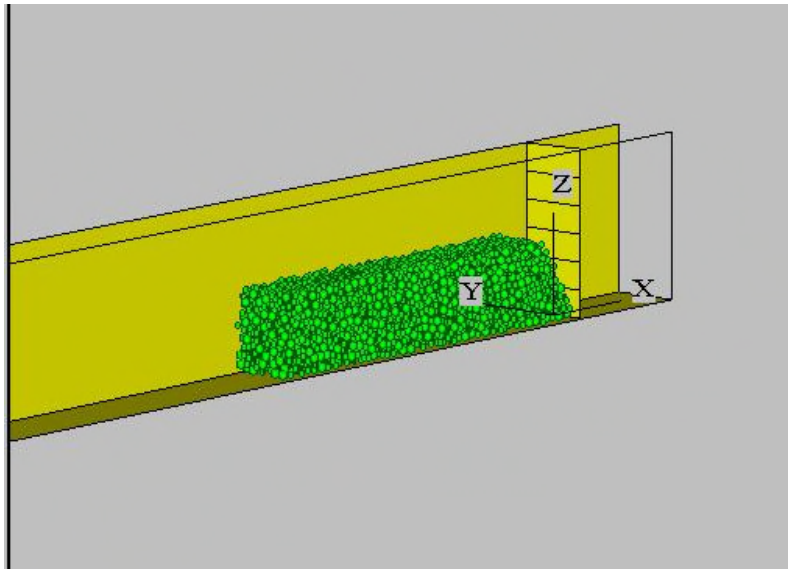

Figure 1: DEM model initial conditions: 3D view of the plain strain model

2. DEM model

The numerical simulations have been performed by employing the PFC 3D code ([16], [17]). For the sake of simplicity, plane strain conditions were externally imposed: the flow width is constant and, to

avoid any dependence of numerical results on it, is equal to eight times the average grain diameter, whereas the friction among grains and side walls was taken equal to 0. The problem geometry taken into consideration is illustrated in Figure 1, where both the rigid barrier and the granular assembly of mass m and initial volume V, are represented. As was previously mentioned, the initial conditions (velocity) for the granular mass are assigned at the instant of time just preceding the impact.

Following the approach proposed in [18] for the quantitative modelling of the soil behaviour, particles are not allowed to rotate and a linear contact stiffness model, characterized by two parameters (k_n and k_s – Table 2) is chosen. Other micro-mechanical parameters that have to be assigned for the system to be modelled are: the inter-particle friction coefficient f_c, the friction coefficient between the grains and the ground and between the grains and the obstacle. The value of f_c=0.3 for the friction among particles was chosen as a typical value for sands/gravels [18], whereas for the grain – wall impact, by assuming an embankment being the "virtual" obstacle, a greater value was chosen (0.6).

In Table 1 the data concerning the initial conditions imposed for the reference test as well as for the model geometry are listed. In Table 2 the micro-mechanical properties are collected.

Table 1: Reference test: Initial conditions and model data

Number of grains	4201
Average grain diameter $\bar{D}$ (m)	0.30
Ratio between the largest and the smallest radius	2.4
Total Volume of grains, V, (m3)	59.4
Length of the grain assembly, ℓ (m)	15
Width of the grain assembly, b (m)	8 $\bar{D}$
Height of the grain assembly h (m)	3
Particle unit weight γ_s (kN/m3)	26
Porosity, por, (-)	0.45
Total Mass m (tons)	154
Initial Average Velocity v_0 (m/sec)	8.73
Initial Kinetic Energy, E_{kin}, (MJ)	5.9
Wall height (m)	6
Front inclination, α, [degrees]	60

Table 2: Reference Micromechanical Properties

$k_n / \bar{D}$ (MPa)	300
$k_s / \bar{D}$ (MPa)	75
Surface friction (ball-ball (f_c); ball-wall; ball-ground; ball-side wall)	0.3; 0.6; 0.3; 0.0

3. Discussion of the numerical results

To clarify the mechanical processes taking place during the impact of the soil mass onto the vertical obstacle, in this sub-section, some phenomenological information are discussed, not only with reference to macro-scopic but even to micro-scopic variables. In particular, in Figure 2 the evolution

of the impact force with time for the reference test is illustrated. The dynamic nature of the process is revealed by the presence of numerous peaks until the attainment of the residual force value. The process is also very rapid; quasi-static conditions are reached in about 1 second.

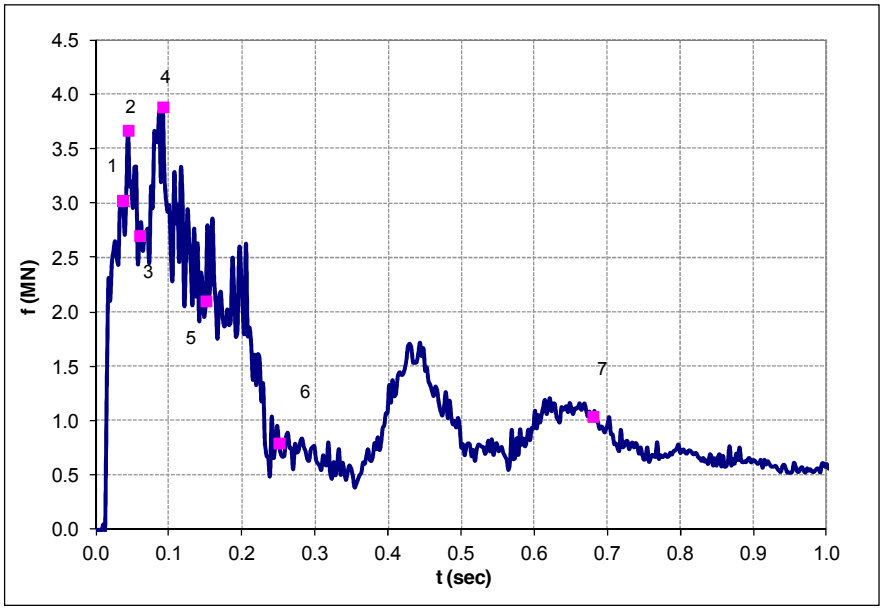

Figure 2: Evolution of the impact force with time for the reference test (Table 1)

In addition, in Figure 3 and Figure 4 the micro-mechanical response of the system is presented by showing the contact forces transmitted by the particles (left) and the velocity vectors (right). Each figure refers to the time instant i (with 1< i <7) of Figure 2. The evolution of the geometry of the soil mass is clearly shown: a marked increase of the effective impact height *H* seems to take place only after point 4 and the maximum height *H* is recorded for i = 7, when the energetic content of the soil mass has already almost totally dissipated. At the peak (point 4), the current *H* value is approximately half of *h*, i.e. the initial flow height of the soil mass.

The intensity of the inter-particle forces (force chains) is normalized with respect to 1 MN in all Figures. This implies that after time instant 4, the forces transmitted by the particles to the obstacle reduce progressively: in fact, owing to the initial geometry of the soil mass, the force concentration is maximum at the initial time instant.

From Figure 3 (d-f) and 4(e-h) it seems evident that in the sub-domain above the red solid lines velocity is characterised by values quite larger than those related to the soil particles positioned below that line. This implies that, below the red line, the soil can be assumed to behave under quasi-static conditions. In contrast, if we take into consideration Figure 3 (a-c) and Figure 4 (a-d), we derive that another frontier can be drawn: this is separating the material behaving like a sort of "granular fluid" from the other part of the mass. In fact, above the light blue straight lines the force chains seem are negligible. In particular, in Figure 3a-c and in Figure 4a,b the forces among particles are negligible in the zone above the light blue line, since that part of the soil mass seems not to be involved in the impact process. In Figure 4c and 4d, the soil mass inside the zone above the light blue line is fluidized, grain velocities are changing direction (most of them are pointing upwards as is evidenced from their relative movement; see also Figures 6, 8) and its agitation is quite relevant: energy is mainly dissipated for impacts and long lasting contacts among particles are almost absent.

The final condition, as is clearly suggested in Figure 4h, is characterized by only two sub-domains, since the blue and the red line are coincident: the material is there either approximately still, below both the drawn lines, or under fluidized conditions, above those lines.

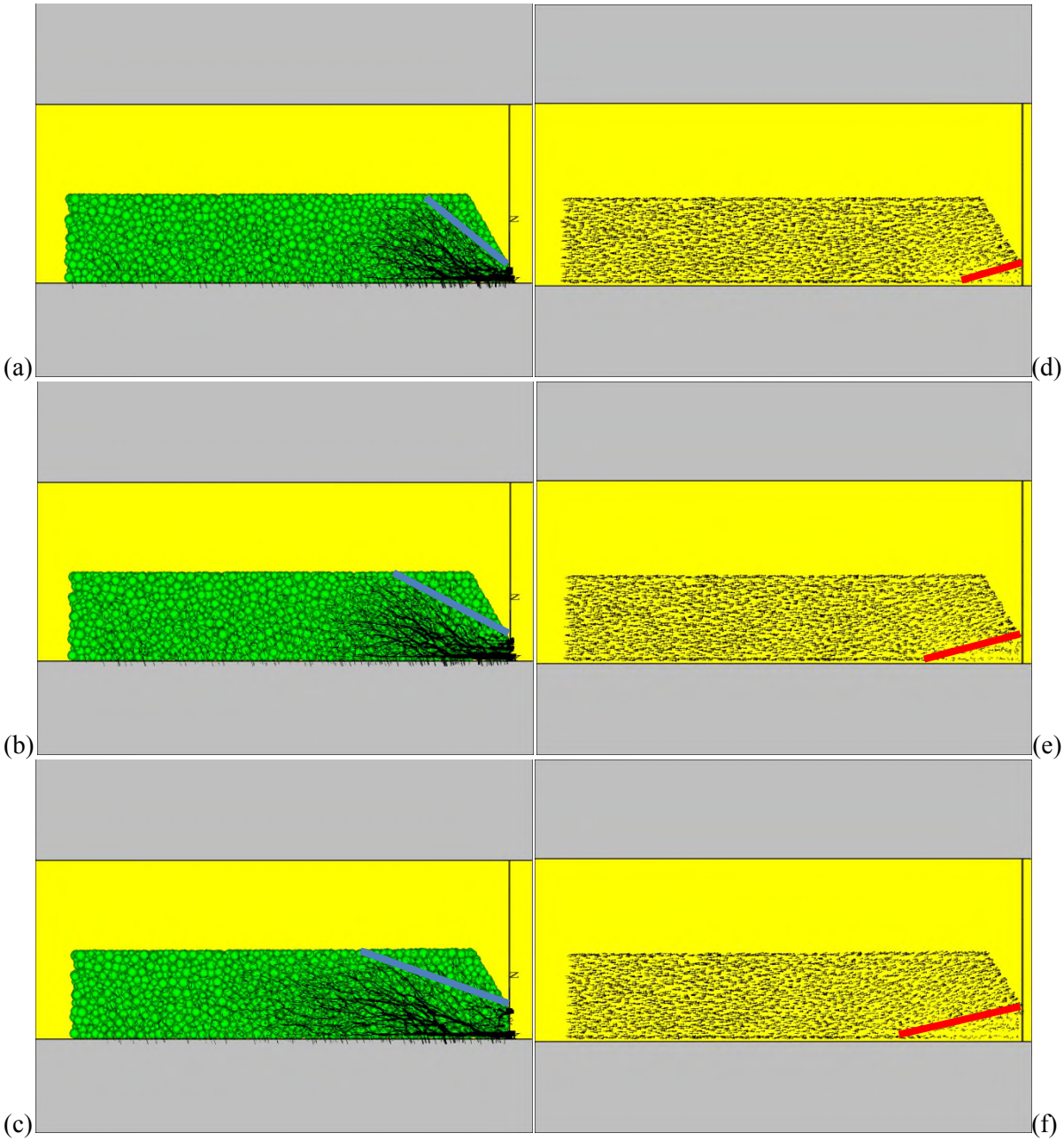

Figure 3: Force chains (left) and velocity vectors (right) during the impact at different time instants: point 1 of Figure 2 (a) and (d), point 2 (b) and (e), point 3 (c) and f).

By summarising, we can state that the impact mechanical process can be described by following the evolution of both the light blue and the red lines, since they subdivide the soil mass in three sub-domains: zone A, in which the soil mass is approximately still (mean velocity is negligible), zone B, in which the material is fluidized and impacts among grains dissipate most of the energy and zone C, which includes the rest of the material; inside this zone, a part of the material behaves like a solid and force chains dominate the mechanical response of the material, whereas some other part remains unaltered with respect to the initial conditions, i.e. this part has not yet participated in the impact.

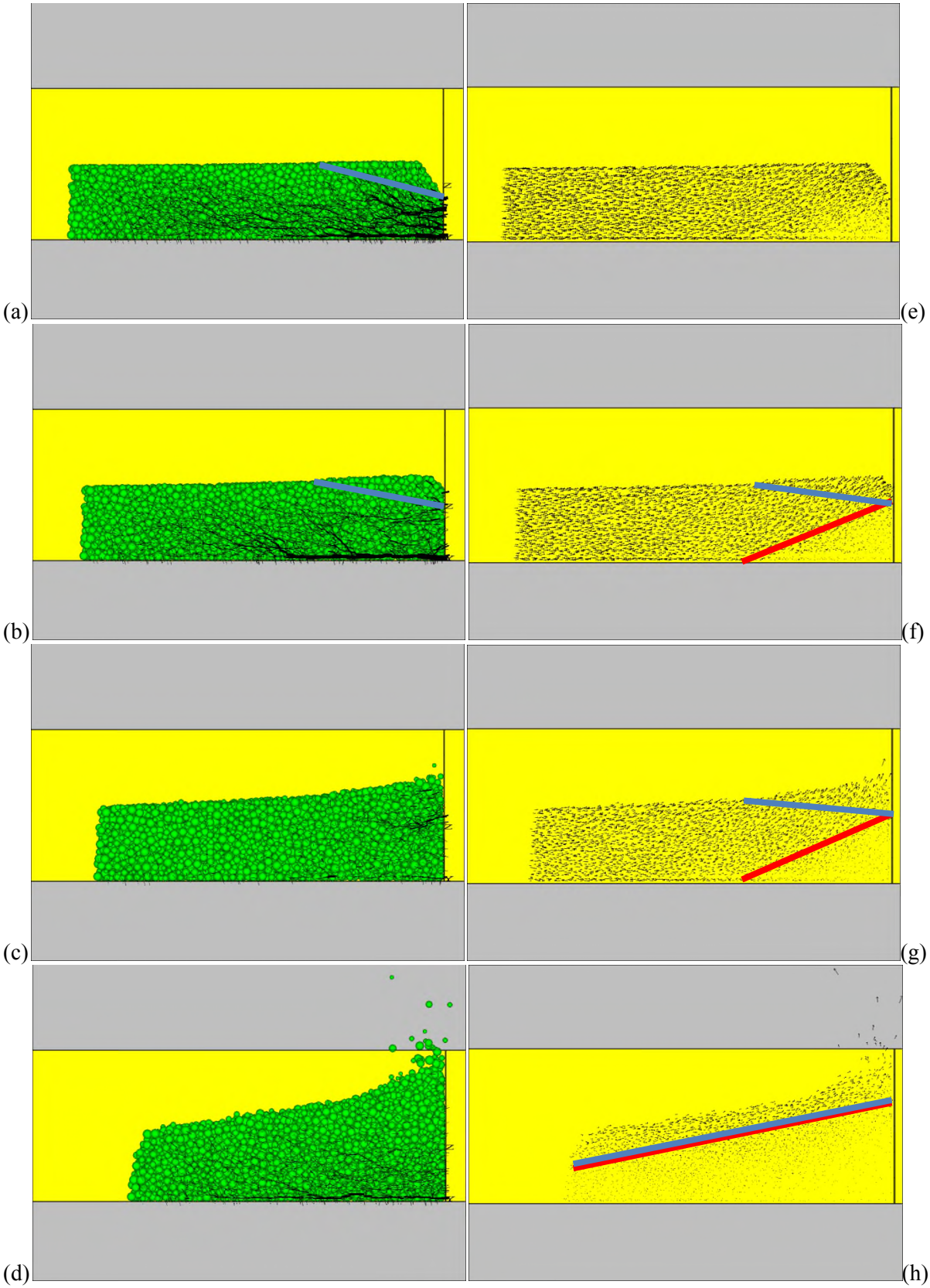

Figure 4: Force chains (left) and velocity vectors (right) at different time instants: point 4 of Figure 2 (a) and (e), point 5 (b) and (f), point 6 (c) and (g), point 7 (d) and (h).

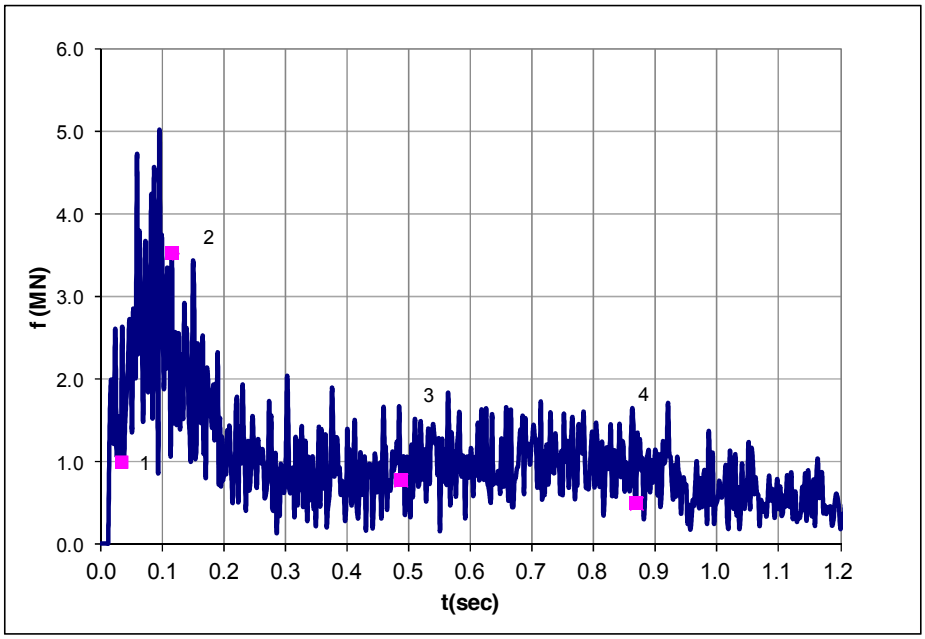

Figure 5: Evolution of the impact force with time in case f_c = 0 and $\alpha = 60°$ (all the other parameters are those of Table 1).

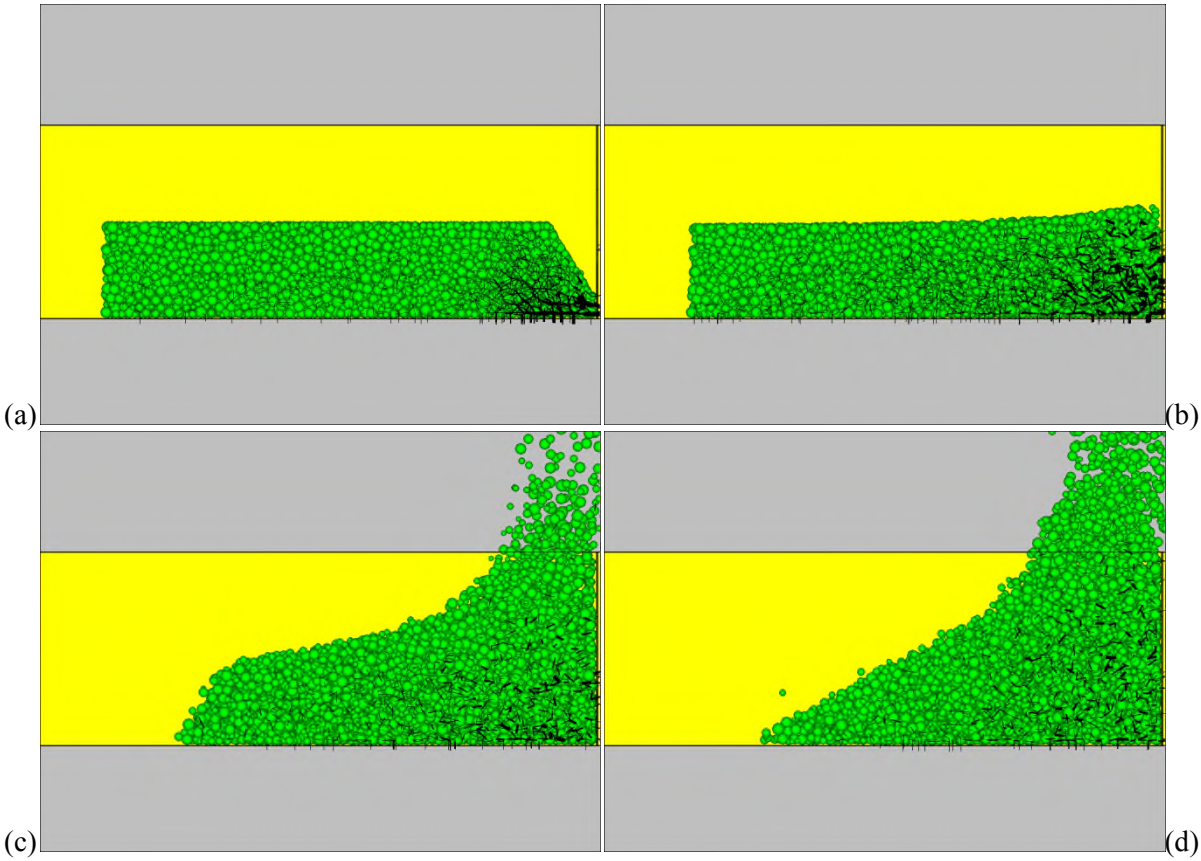

Figure 6: Force chains (black lines) within the soil mass during the impact at different time instants: point 1, 2, 3, 4 of Figure 5 correspond to (a), (b) (c) and (d) respectively.

To emphasize the role played by the parameters f_c and α in influencing the mechanical response of the soil mass, in Figures 5-10, analogous results concerning contact forces only (due to space

limitations) are shown. Figures 5 and 6 present the tests with $f_c = 0$ and $\alpha = 60°$, while Figures 7 and 8 refer to the micromechanical evolution of the test with $f_c = 0$ and $\alpha = 90°$. Finally the results of the test concerning $f_c = 1$ and $\alpha = 90°$ are also shown in Figure 9 and Figure 10.

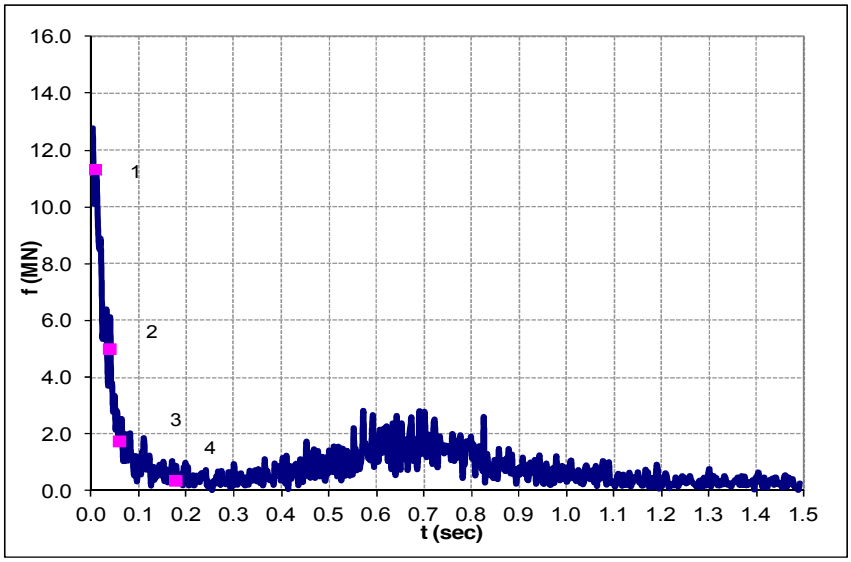

Figure 7: Evolution of the impact force with time in case $f_c = 0$ and $\alpha = 90°$ (all the other parameters are those of Table 1).

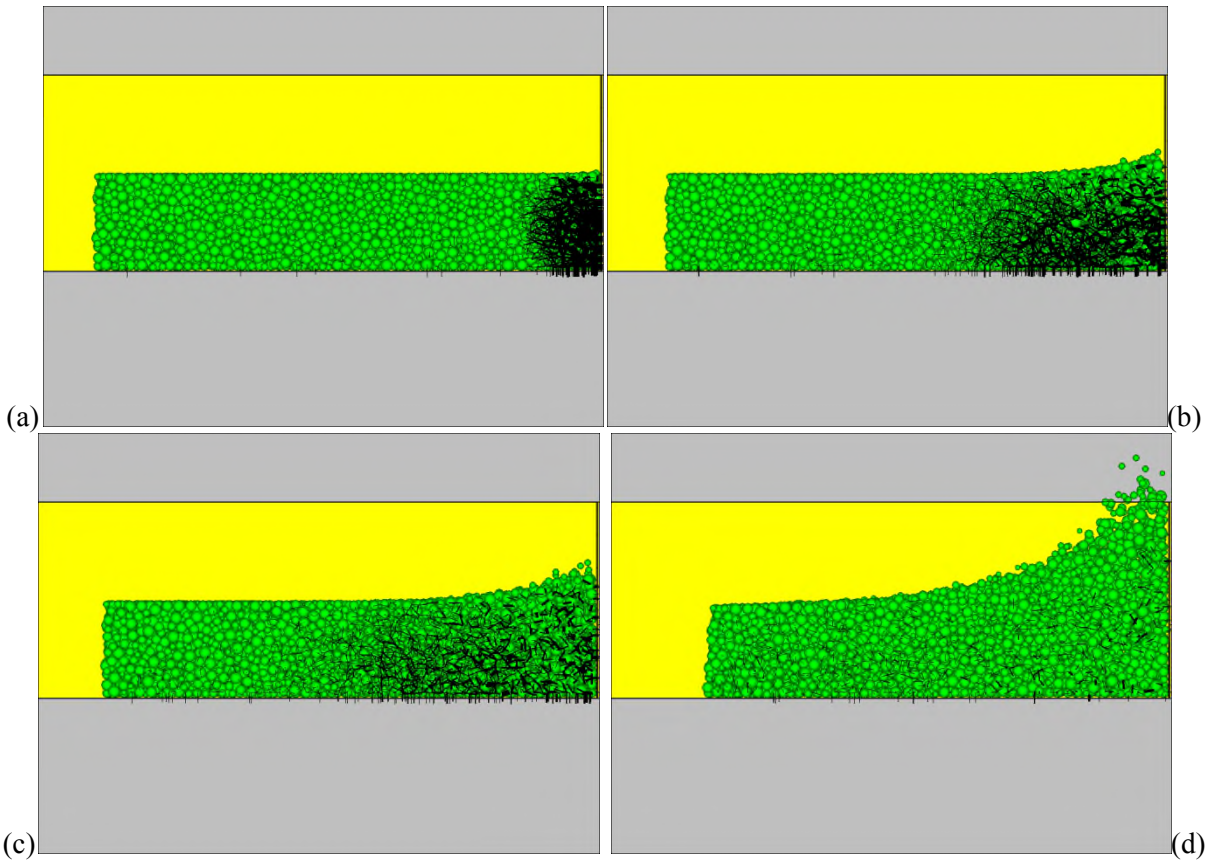

Figure 8: Force chains (black lines) within the soil mass during the impact at different time instants: point 1 of Figure 9 (a), point 2 (b), point 3 (c) and point 4 (d)).

For $f_c = 0$ and $\alpha = 60°$, (Figures 5, 6) the evolution of the impact force with time is more irregular than in the reference case. Moreover, part of the mass overtakes the obstacle, and force chains during the impact are practically absent and the mass appears to be totally fluidized (Figure 6). By changing only the front inclination, i.e. with $f_c = 0$ and $\alpha = 90°$, (Figures 7, 8) the force – time graph shows that the soil mass behaviour is more solid-like, initially; in fact the MIF is significantly increased and it develops very fast; then a force wave propagation starts spreading backwards, although it is vanishing very rapidly. After some time instants a fully fluidised behaviour is developed inside the whole mass, similar to the behaviour observed in a previous test (Figure 6c,d compared to Figure 8d).

In contrast, when f_c=1 and $\alpha = 90°$, the material seems to behave like a solid throughout the test: (a) the MIF is larger than the value corresponding to α=60° and (b) it is attained at a time instant very close to t=0, that is immediately after the impact (Figure 9). In this test the force propagation wave is more evident: in Figure 10b the force wave is travelling backward and has reached the backward boundary of the soil mass, in Figure 10c and d the force wave is travelling towards the barrier, until its nullification that is evident in Figure 10e (when impact force goes to zero). Again, in the most superficial part of the soil mass the force chains seem to be absent and the velocity fluctuations more pronounced.

By comparing the two last tests we can conclude that the front inclination and the inter-particle friction are influencing very much the overall behaviour of the soil mass. Nevertheless, the parameter which dominates the solid/fluid like behaviour of the mass is the inter-particle friction: when the inter-particle friction angle value is sufficiently large, the soil mass seems to prevalently behave like a solid.

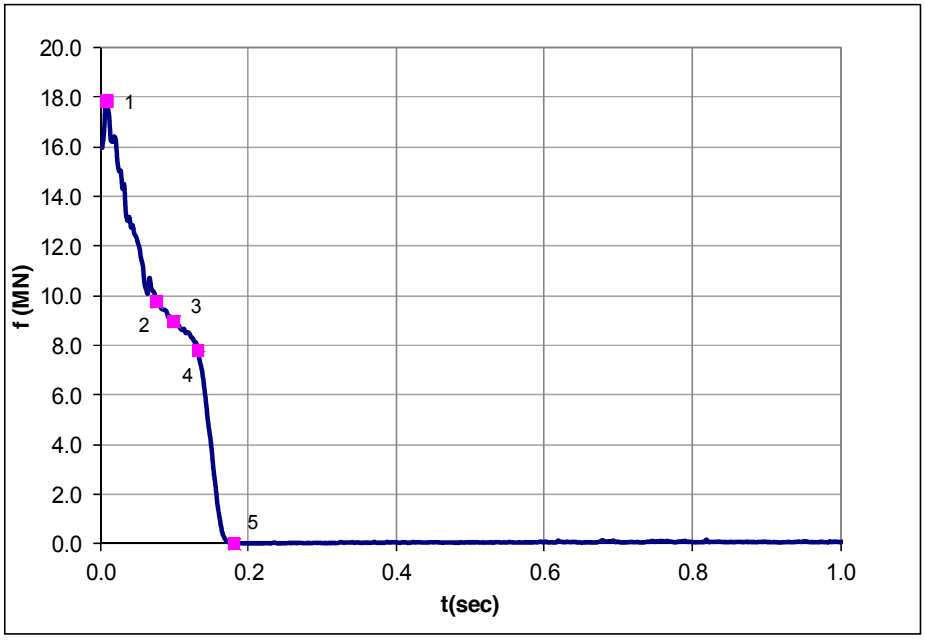

Figure 9: Evolution of the impact force with time in case f_c = 1 and $\alpha = 90°$ (all the other parameters are those of Table 1).

4. Conclusions

In this paper the impact of dry granular masses on rigid barriers is analysed. In particular, the authors illustrated some numerical results, putting in evidence from a qualitative point of view the nature of the mechanical process.

The numerical results were obtained by using a commercial DEM code. The soil mass impact has been described by analysing the evolution with time of the impact force, of the force chains and of the velocity field within the granular mass. Three different values of the inter-particle friction angle were taken into account to emphasize the double nature of the mechanical behaviour of the material that, during the impact, this seems to behave partially like a solid and partially like a granular fluid.

In particular, when the inter-particle friction angle is sufficiently small, the system tends to behave like a fluid, whereas when the inter-particle friction angle value is sufficiently large, the soil mass seems to prevalently behave like a solid. When the front inclination is large, some aspects of the solid-like behaviour are visible even for small values of inter-particle friction.

In contrast, when the inter-particle friction angle is intermediate, during the impact, part of the soil mass seems to behave like a solid and in the more superficial zone like a fluidized mass. To schematize the overall behaviour of the soil mass, three zones develop during impact: in one the material is approximately still, in another one the agitation governs the material response. The geometry of the three zones evolves with time: the first and the second one progressively increase, whereas the third one disappears at the end of the dynamic process.

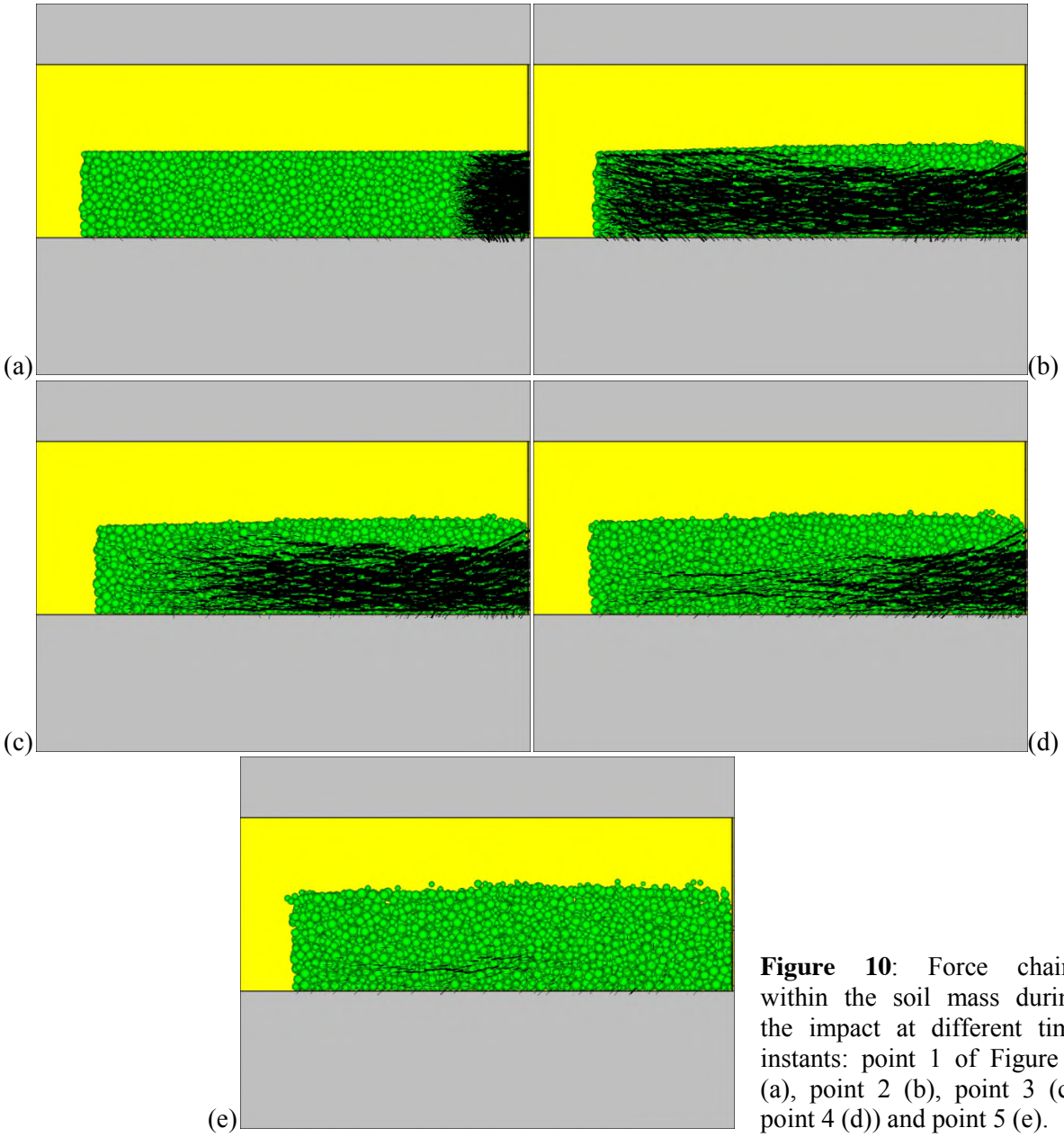

Figure 10: Force chains within the soil mass during the impact at different time instants: point 1 of Figure 9 (a), point 2 (b), point 3 (c), point 4 (d)) and point 5 (e).

5. Acknowledgments

This research was financially supported by the Italian government within the framework of PON01_01869 Project "Tecnologie e Materiali Innovativi per la Difesa del Territorio e la Tutela dell'ambiente" and of the PRIN 2011 Project titled "La mitigazione del rischio da frana mediante interventi sostenibili".

6. References

[1] Hübl J, Suda J, Proske D, Kaitna R, Scheidl C. Debris flow impact estimation. *Eleventh international symposium on water management and hydraulic Engineering* 2009 137–48.
[2] Ishikawa N, Inoue R, Hayashi K, Hasegawa Y and Mizuyama T Experimental Approach on measurement of impulsive fluid force using debris flow model *Conference proceedings interpraevent* 2008 343–54.
[3] Armanini A 1997 *On the dynamic impact of debris flows*. Recent Dev Debris Flows (Berlin: Springer)
[4] Suda J, Hübl J, Bergmeister K Design and construction of high stressed concrete structures as protection works for torrent control in the Austrian Alps *Proceedings of the third international fib congress* 2010 1–12.
[5] Dok L 2000 *Review of Natural Terrain Landslide Debris-resting Barrier Design* (Hong - Kong: Civil Engineering Department: Government of the Hong Kong Special Administrative Region), 123.
[6] Kwan JSH 2012 *Supplementary Technical Guidance on Design of Rigid Debris-resisting Barriers*. *GEO Technical Note No*. *TN 2/2012 (GEO Report No*. *270),* (Hong Kong: The Government of the Hong Kong Special Administrative Region)
[7] Arattano M, Franzi L. On the evaluation of debris flows dynamics by means of mathematical models *Nat Hazards Earth Syst Sci* 2003 **3(6)** 539–44.
[8] Jóhannesson T, Gauer P, Issler P and K. Lied K (Eds) 2009 *The design of avalanche protection dams, Recent practical and theoretical developments*. (Brussels: European Comission) Climate Change and Natural Hazard Research - Series 2 Project report EUR 23339, DOI: 10.2777/12871.
[9] Huang, HP, Yang, KC, and Lai SW Impact force of debris flow on filter dam *Geophysical Research Abstracts* 2007 **9** 03218.
[10] Miyoshi I. Experimental Study of Impact Load on a Dam Due to Debris Flow. *Proceedings of the IUFRO Technical Session on Geomorphic Hazards in Managed Forests*. *Pacific Southwest Research Station* 1990 90.
[11] Salciarini D, Tamagnini C, Conversini P. Discrete element modeling of debris-avalanche impact on earthfill barriers *Phys Chem Earth, Parts A/B/C* Elsevier Ltd 2010 **35(3-5)** 172–81.
[12] Li X, He S, Luo Y, and Wu Y Discrete element modeling of debris avalanche impact on retaining walls *Journal of Mountain Science* 2010 **7(3)** 276-281.
[13] Spang R M 1998 Rockfall Barriers-Design and Practice in Europe *Proceedings of the Seminar on Planning, Design and Implementation of Debris Flow and Rockfall Hazards Mitigation Measures* 1-8.
[14] Yoshida H Recent experimental studies on rockfall control in Japan *Proc*. *of the Joint Japan-Swiss Scientific Seminar on Impact Load by Rock Falls and Design of Protection Structures* 1999 69-78.
[15] Calvetti F, di Prisco C and Vairaktaris E DEM numerical assessment of impact forces of dry granular masses on rigid barriers. *Acta Geotechnica* 2015 (submitted for publication)
[16] Cundall P A and Strack O D A discrete numerical model for granular assemblies. *Geotechnique*, **29(1)** 47-65.

[17] Cundall PA and Hart RD Numerical modelling of discontinua. *Engineering computations* 1992 **9(2)** 101-113.
[18] Calvetti F Discrete modelling of granular materials and geotechnical problems *European Journal of Environmental and Civil Engineering* 2008 **12(7-8)** 951-965.
[19] Calvetti F, di Prisco C and Vairaktaris E DEM modeling of soil/rock avalanche impact on barriers, *Int. J. Numer. Anal. Meth. Geomech.* 2015 (to be submitted for publication)